



HAL
open science

Improving past sea surface temperature reconstructions from the Southern Hemisphere oceans using planktonic foraminiferal census data

N.A. Haddam, Elisabeth Michel, G. Siani, G. Cortese, H.C. Bostock, J.M Duprat, G. Isguder

► To cite this version:

N.A. Haddam, Elisabeth Michel, G. Siani, G. Cortese, H.C. Bostock, et al.. Improving past sea surface temperature reconstructions from the Southern Hemisphere oceans using planktonic foraminiferal census data. *Paleoceanography*, 2016, 31 ((6):), pp.822-837 (IF 3,738). 10.1002/2016PA002946 . hal-01417373

HAL Id: hal-01417373

<https://hal.science/hal-01417373>

Submitted on 9 Oct 2020

HAL is a multi-disciplinary open access archive for the deposit and dissemination of scientific research documents, whether they are published or not. The documents may come from teaching and research institutions in France or abroad, or from public or private research centers.

L'archive ouverte pluridisciplinaire **HAL**, est destinée au dépôt et à la diffusion de documents scientifiques de niveau recherche, publiés ou non, émanant des établissements d'enseignement et de recherche français ou étrangers, des laboratoires publics ou privés.



Paleoceanography

RESEARCH ARTICLE

10.1002/2016PA002946

Key Points:

- A new Southern Hemisphere planktonic foraminifera database compilation for SST
- Improved precision of paleo-SST reconstructions by reducing dissolution biases in SHO core tops
- Improved SST reconstructed for core MD07-3100 using SHO database with the modern analog technique

Supporting Information:

- Supporting Information S1
- Table S2
- Table S3
- Table S4

Correspondence to:

N. A. Haddam,
naoufel.haddam@lsce.ipsl.fr

Citation:

Haddam, N. A., E. Michel, G. Siani, G. Cortese, H. C. Bostock, J. M. Duprat, and G. Isguder (2016), Improving past sea surface temperature reconstructions from the Southern Hemisphere oceans using planktonic foraminiferal census data, *Paleoceanography*, 31, 822–837, doi:10.1002/2016PA002946.

Received 7 MAR 2016

Accepted 27 MAY 2016

Accepted article online 5 JUN 2016

Published online 27 JUN 2016

©2016. American Geophysical Union.
All Rights Reserved.

Improving past sea surface temperature reconstructions from the Southern Hemisphere oceans using planktonic foraminiferal census data

N. A. Haddam^{1,2}, E. Michel², G. Siani¹, G. Cortese³, H. C. Bostock⁴, J. M. Duprat⁵, and G. Isguder²

¹GEOPS Geosciences Paris-Sud, CNRS, Université de Paris Sud, Orsay, France, ²LSCE/IPSL Laboratoire des Sciences du Climat et de l'Environnement, CEA-CNRS-UVSQ, Gif-sur-Yvette, France, ³GNS Science, Lower Hutt, New Zealand, ⁴National Institute of Water and Atmospheric Research, Wellington, New Zealand, ⁵EPOC, Université de Bordeaux, Talence, France

Abstract We present an improved database of planktonic foraminiferal census counts from the Southern Hemisphere oceans (SHO) from 15°S to 64°S. The SHO database combines three existing databases. Using this SHO database, we investigated dissolution biases that might affect faunal census counts. We suggest a depth/ ΔCO_3^{2-} threshold of $\sim 3800 \text{ m}/\Delta\text{CO}_3^{2-} = \sim -10$ to $-5 \mu\text{mol/kg}$ for the Pacific and Indian Oceans and $\sim 4000 \text{ m}/\Delta\text{CO}_3^{2-} = \sim 0$ to $10 \mu\text{mol/kg}$ for the Atlantic Ocean, under which core-top assemblages can be affected by dissolution and are less reliable for paleo-sea surface temperature (SST) reconstructions. We removed all core tops beyond these thresholds from the SHO database. This database has 598 core tops and is able to reconstruct past SST variations from 2° to 25.5°C, with a root mean square error of 1.00°C, for annual temperatures. To inspect how dissolution affects SST reconstruction quality, we tested the data base with two “leave-one-out” tests, with and without the deep core tops. We used this database to reconstruct summer SST (SSST) over the last 20 ka, using the Modern Analog Technique method, on the Southeast Pacific core MD07-3100. This was compared to the SSST reconstructed using the three databases used to compile the SHO database, thus showing that the reconstruction using the SHO database is more reliable, as its dissimilarity values are the lowest. The most important aspect here is the importance of a bias-free, geographic-rich database. We leave this data set open-ended to future additions; the new core tops must be carefully selected, with their chronological frameworks, and evidence of dissolution assessed.

1. Introduction

Past climate data provide the opportunity to test our understanding of climate feedbacks, thresholds, and nonlinear responses to forcing variables. Moreover, these data are necessary to evaluate the performance of climate models. One of the most important climate variables is sea surface temperature (SST), and hence, many proxies have been developed and used for its reconstruction from past geological archives (see *Mix et al.* [2001] for a review), e.g., Mg/Ca ratio in foraminiferal carbonate tests [*Nürnberg*, 1995]; Uk'37 (unsaturation index) of alkenone chains [*Brassell et al.*, 1986]; and transfer functions based on census counts of planktonic organisms, including planktonic foraminifera [*Imbrie and Kipp*, 1971; *Pflaumann et al.*, 1996; *Malmgren and Nordlund*, 1996]. However, an intercomparison of results from these different SST reconstruction methods highlighted considerable discrepancies [*Bard*, 2001], suggesting that a better understanding and calibration of each proxy is necessary.

Planktonic foraminiferal assemblages are one of the most commonly used proxies for paleo-temperature reconstructions due to the close dependence between their species abundances and the physicochemical variables of their habitats [*Kucera et al.*, 2005a]. A study in the North Atlantic has shown that paleo-SST reconstructions obtained from foraminiferal assemblages showed the best agreement with climate models, compared to other paleo-SST proxies [*Caley et al.*, 2014].

Imbrie and Kipp [1971] developed a transfer function for planktonic foraminifera to obtain quantitative reconstructions of SST. Subsequently, the Modern Analog Technique (MAT) was developed, which has proven to be amongst the most accurate reconstruction methods [*Prell*, 1985]. Unlike other transfer function methods, to estimate the SST, MAT takes into account rare species, not only the most abundant ones. MAT can also provide a reconstruction even when the relationship between the species and the environmental parameter are nonlinear [*Kucera et al.*, 2005a]. The MAT method directly measures the distance between the planktonic

foraminifera faunal composition of a fossil sample with the assemblages from a modern core-top database, and it identifies the best set of modern analogs [Prell, 1985].

In order to be able to generate MAT SST reconstructions for paleoclimate studies, many core-top databases have been compiled and extensively tested. In the Atlantic Ocean, where many core tops are available, these databases have proven to be very effective for reconstructing SST [Pflaumann *et al.*, 1996; Kucera *et al.*, 2005a]. In the past, there has only been a limited number of core tops available for the Southern Hemisphere oceans (SHO), and the current databases [Cortese *et al.*, 2013; MARGO: Kucera *et al.*, 2005a] need to be extensively tested. Given the importance of the Southern Ocean (SO) in the climate system [Marshall and Speer, 2012], we have compiled a new, improved, core-top database for the SHO. This database will be useful to produce improved SHO paleo-SST reconstructions.

This study aims to provide a modern database that is “as free as possible” from various sources of bias (e.g., statistical significance of species counts, coastal influence on planktonic foraminiferal assemblages, effects of selective dissolution, and nonmodern samples), that will reduce the quality of environmental estimates. The improved paleo-SST precision will allow for model simulation/paleo data comparisons and better insights in to the potential climatic mechanisms. This paper will discuss how the new SHO core-top database was compiled and propose strict criteria for the inclusion of future core tops. This database is then tested and validated using the leave-one-out test, with and without deep core tops, to assess the reconstruction quality of the SST. We then used the database to reconstruct SST over the last 20 ka by applying the MAT method to planktonic foraminifera census data from a marine sediment core MD07-3100, retrieved from the Southeast Pacific (SEP), and the obtained SST are compared to SST reconstructed with the previously available databases.

2. Development of the New Modern Core-Top Database

The ideal analog database for SST reconstructions should be composed of recent core tops, with assemblages based on census counts of a minimum of 300 individuals for the best statistical representation of species that have a relative abundance of at least 10% [Patterson and Fishbein, 1989]. Furthermore, the assemblages of these core tops should ideally be mainly influenced by oceanic SST. However, foraminifera assemblages are often affected by other influences, for example, the selective dissolution of certain species [e.g., Thunell, 1976] which affects many deep-sea core tops. To meet these requirements, we perform a quality check on the core tops to be included in the database, to improve the reliability of the derived SST reconstructions for the SO. Therefore, this paper focuses on the compilation of the best quality core tops for SST reconstruction in the SHO.

This new database extends from 15°S, at the northern limb of the middle- to low-latitude gyres in the Atlantic, Indian, and Pacific Oceans to the coast of Antarctica, to allow the reconstruction of past latitudinal variations of the polar, subpolar, and subtropical waters. The SHO is separated into three main sectors; Atlantic, Indian, and Pacific basins. In general, better SST reconstructions will be obtained by using a core-top database from the same geographical area as the same genetic species will be considered [Pflaumann *et al.*, 1996; Kucera *et al.*, 2005a]. Indeed, the occurrence of cryptic species of protists in the World Ocean [de Vargas *et al.*, 1999; Darling *et al.*, 2004; Darling and Wade, 2008] has the potential to introduce errors in species determination, as the taxonomy of the various types of protists is based on morphology (i.e., their skeletal remains), rather than their genotype. In our study area, the SHO, we expect the organisms to be very well mixed by the Antarctic Circumpolar Current (ACC) system, which mitigates the problem with cryptic species and allows us to assume that the same genetic species are likely to occur in all three sectors.

The annual and/or seasonal modern climatological temperatures (average of 30 years) are associated with each core top in the database. The paleo-SST of the fossil assemblage is the mean of the SST of the nearest analogs. The degree of similarity between a fossil sample and the best modern analogs is estimated using a square chord distance test (dissimilarity coefficient) [Prell, 1985]. The lower the dissimilarity is, the more reliable the reconstructed SST will be. A dissimilarity coefficient threshold of 0.25 has often been used, under which the SST reconstructions were considered to be of good quality [Prell, 1985; Kallel *et al.*, 2000]. However, dissimilarity is also a function of the faunal diversity, as dissimilarity values increase with diversity, thus displaying higher values in low latitudes compared to high latitudes [Waelbroeck *et al.*, 1998]. Thus, we have not used a specific dissimilarity threshold in this study.

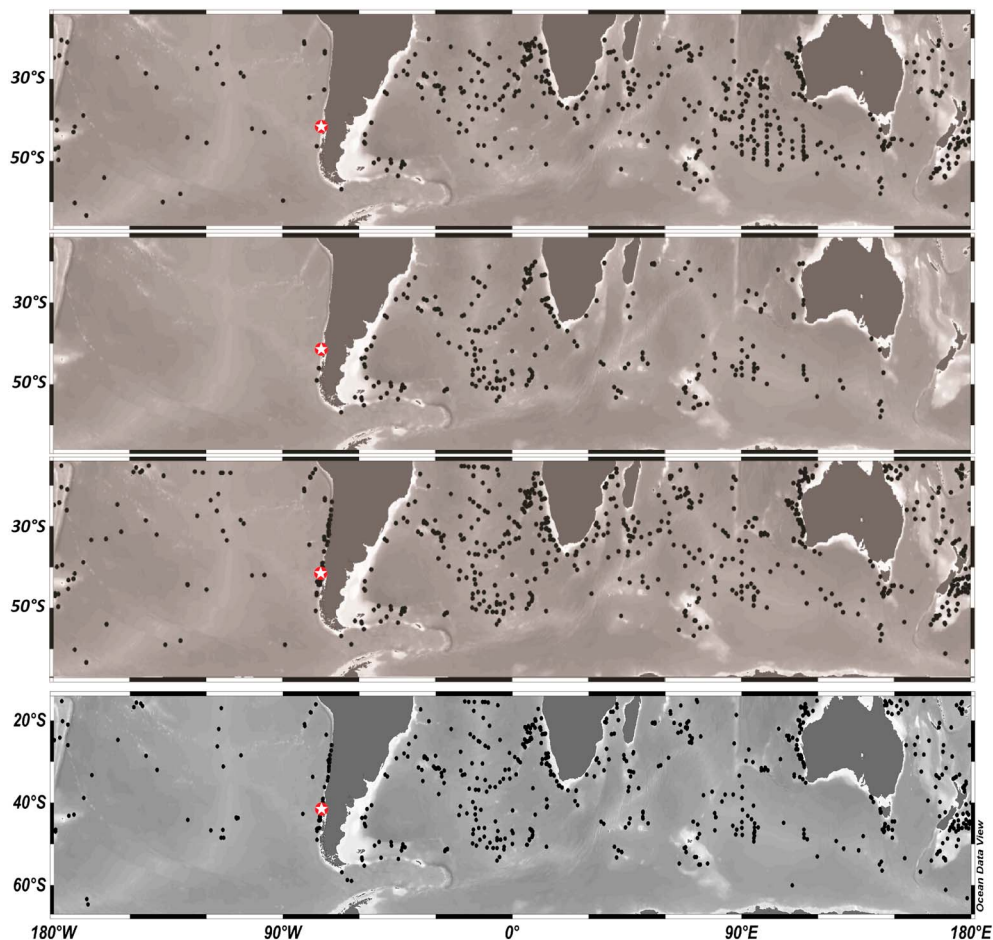


Figure 1. Map of core tops compiled in the different databases. (first panel) The MARGO database; (second panel) the French database; (third panel) Cortese' database, and (fourth panel) the new SHO database. The star represents the location of core MD07-3100.

2.1. Database Compilation

We compiled three existing core-top databases, (i) the MARGO project database covering the Atlantic, Indian, and Pacific Oceans, cut at 15°S and containing 550 core tops [Kucera et al., 2005a], hereafter named the MARGO database; (ii) a recently published database containing 771 core tops [Cortese et al., 2013], hereafter named the Cortese database; and (iii) an unpublished database from the Atlantic and Indian sectors of the SO based on Salvignac [1998] with additional core tops from the South Atlantic, Pacific, and Indian Oceans (Gif/Orsay database), containing 261 core tops, hereafter named the French database. The new compiled database is called the SHO database, with core tops from 15°S to 64°S. Compiling these three databases provides an improved coverage of the Pacific Ocean especially along the Peruvian and Chilean margin in the SEP (Figure 1).

Foraminifera counts in these databases were made in the >150 μm fraction; this would lead to an underestimation of taxa with smaller tests. The total number of taxa in the new compilation is 35. Several species, or subspecies, in our new database were combined (supporting information Table S1). We combined *Globigerinoides sacculifer* and *G. trilobus* following the same approach as the Cortese database [Cortese et al., 2013]. This is unlikely to be an issue as these two ontogenetic growth types share the same ecological niches and thus provide the same SST range [Bé, 1977; Niebler and Gersonde, 1998]. *G. ruber* white and the chromotype *G. ruber* pink [Aurahs et al., 2011] are also combined in the Cortese database despite the fact that they do not share the same optimal range of temperature. However, this is unlikely to be a significant problem as within the MARGO and the French databases there are only ~50 cores containing individuals of *G. ruber* pink in their assemblages, among which only three low-latitude cores have >5% of this subspecies.

Following this logic, for the databases where intergrade forms between *Neogloboquadrina dutertrei* and *N. pachyderma* right coiling were considered in separated counts, we have been compelled to combine them with *N. pachyderma* right coiling counts. This combination might artificially broaden the SST range of *N. pachyderma* right coiling as the intergrade form grows under slightly warmer SST [Pflaumann et al., 1996]. Lastly, we combined *Globorotalia menardii*, *G. tumida*, and *G. flexuosa* as they were not counted separately in the Cortese database. For the first two species, both thrive in the same temperature range of 19 to 28°C [Pflaumann et al., 1996], while *G. flexuosa* has been associated with fertile upwelling zones [Cullen and Prell, 1984].

During this compilation we applied a rigorous quality control of the core tops, checking the available voyage and campaign reports. This allowed several errors on the longitude, latitudes, depth, and even station names to be corrected on ~100 core tops across the different databases. We have also quality controlled the chronological information provided for the core tops where available. We reused the chronology information available in the MARGO database and ranked the cores of the remaining databases, following the MARGO notation with five levels: (i) level 1, chronologic control based on radiometric dating (e.g., U/Th and reservoir-corrected ¹⁴C) indicating an age < ~2000 years; (ii) level 2, chronologic control established by any kind of radiometric date indicating an age < ~4000 years or stained benthic foraminifera with sedimentation rate higher than 5 cm/ka; (iii) level 3, Any kind of radiometric date between 4000 to 8000 years or a specific stratigraphic control (e.g., extinction or emergence of a species) indicating an age < ~4000 years; (iv) level 4, stratigraphic constrained (as δ¹⁸O stratigraphy and CaCO₃ percentages) indicating an age < ~4000 years; and (v) level 5, no age control available for the core top [see Kucera et al., 2005b]. Unfortunately, 85% of the core tops in the databases display a level 5 chronology. It is very likely that core tops from low sedimentation areas would not be recent and may be >8000 years or older. This may bias the paleo-SST reconstruction if these core tops were to be chosen as analogs.

We also excluded the core tops shallower than ~500 m in the three databases, because planktonic foraminiferal assemblages from the coastal environments are more likely to be influenced by factors other than SST [Pflaumann et al., 1996].

2.2. Dissolution-Biased Core Tops

Species-selective dissolution can affect deep core-top faunal composition both above [Volbers and Henrich, 2002] and below the lysocline [Arrhenius, 1952; Berger, 1970; Phleger et al., 1953; Ruddiman and Heezen, 1967; Schott, 1935; Thunell, 1976]. This bias in the faunal composition precludes reliable paleo-SST reconstructions. Selective dissolution will first affect test weights of fragile species without destroying the whole shell. However, once dissolution starts to affect the abundance of dissolution-sensitive species shells, the whole planktonic foraminiferal assemblage will be biased. Thus, in order to find out which core-top assemblages are biased by dissolution, we propose a “dissolution” criterion. Carbonate dissolution is enhanced with increasing water depth (pressure) and decreasing carbonate concentration [ΔCO_3^{2-}], i.e., the undersaturation of the bottom waters toward calcite. In the following discussion, we will use the ΔCO_3^{2-} notation to signify the difference between in situ [ΔCO_3^{2-}] concentration and the calcite horizon saturation concentration at the depth the cores were retrieved following the equations of Broecker and Takahashi [1978]:

$$\Delta\text{CO}_3^{2-} (\mu\text{M}/\text{kg}) = [\text{CO}_3^{2-}] - [\text{CO}_3^{2-}]_{\text{cc}} \quad \text{and} \quad [\text{CO}_3^{2-}]_{\text{cc}} = 90\exp(0.16(Z - 4)) \quad (1)$$

where [ΔCO_3^{2-}]_{cc} is the critical concentration for calcite and Z is the water depth of the core in kilometers.

To eliminate any dissolution bias, we used two different approaches: (1) an evaluation of the changes observed in the percentages of sensitive to resistant foraminiferal species (see next paragraph) with depth and (2) an examination of planktonic foraminiferal assemblage dissimilarities along bathymetric core-top transects. Information on the relative abundance of planktonic foraminifera fragments (fragmentation index, *Le and Shackleton* [1992]) in the core top would provide an alternative indicator of possible dissolution. Unfortunately, no fragmentation data were available to use in this study.

For the first approach, we separated each basin (Atlantic, Indian, Pacific, and SO for the cores south of the Polar Front) and the upwelling zones, into 5°C zones using World Ocean Atlas 1998 summer SST [Conkright et al., 1998]. We then analyzed the faunal contents of the core tops by grouping the most abundant species according to their resistance to dissolution following Cullen and Prell’s classification [Cullen and Prell, 1984].

For resistant species percentages (RSP), we added together the percentages of *Globorotalia inflata*, *G. flexuosa*, *G. menardii*, *G. tumida*, *N. dutertrei*, and *Pulleniatina obliquiloculata*. For moderately resistant species percentages (MSP), we added the percentages of *Globigerinella siphonifera*, *G. conglobatus*, and *Globoquadrina conglomerata*. For sensitive species (SS), we summed the percentages of *G. ruber*, *Globigerina bulloides*, and *Globigerinina glutinata*. The only difference between our classification and Cullen and Prell's is to exclude *N. pachyderma* (both left and right coiling). Indeed, Cullen and Prell's classification was based on studies from tropical regions, where there are few *N. pachyderma* forms. At higher latitudes the assemblages are dominated by *N. pachyderma* forms, which will overwhelm the effects of dissolution on the foraminiferal assemblages.

We plotted the percentages of these three groups (RSP, MSP, and SS) in each 5°C range (from 0 to 30°C, except in the Indian sector where the first grouping is for 8–15°C, as there are less than 10 core tops between 8 and 10°C) to limit their SST dependency. For the three oceanic basins, the percentages of each group are plotted against depth to evaluate the threshold at which planktonic foraminiferal assemblages start to be biased by dissolution (Figure 2). The major pattern observed is the increase in RSP percentage with depth, sometimes associated with a decrease in SS percentage (Figures 2d, 2g, 2h, 2i, and 2k). The RSP percentage maxima are generally lower for high temperatures (25–30°C) and low temperatures (<15°C), at depths <3000 m, than for the intermediate temperature ranges (10–15 and 15–20°C).

In the 10–15°C and 25–30°C ranges in the Pacific Ocean (Figures 2a and 2j), the RSP are lower than 20–25% for shallow cores. The only exception is a core at ~2000 m with a RSP >30% (Figure 2j). This core is potentially affected by supralysocline dissolution due to higher organic matter fluxes at this location. At depths >4000 m we observe an increase in RSP in all regions, potentially indicating dissolution-biased counts. In the Atlantic Ocean, for the 25–30°C range, the RSP are lower than 20–25% at all depths, down to 4700 m. In the Indian Ocean, in the 25–30°C range, the percentage of the RSP increases to >35% for cores deeper than 4000 m, probably as a result of dissolution-biased assemblages. In the 8–15°C range (Figure 2b), a number of cores have RSP percentages of ~40%, and there is no obvious increase of the RSP with depth, except for the deepest core with a RSP content >55%. More core tops from deeper depths will be required to define a potential threshold depth for dissolution impacting planktonic foraminifera assemblages in this region.

Within the range of 15–25°C, for all the basins (Figures 2d, 2e, 2f, 2g, 2h, and 2i), we observe higher RSP values, from 20 to >50%, at all depths. This widespread response might be due to ecological factors, as this range is transitional, including both cool- and warm-water species, and the RSP percentages in this range are dominated by the presence of *G. inflata*, *G. menardii* spp., and *N. dutertrei*. However, there is still an increase in the RSP species percentages at depths >3600 and ~3000 m for the Pacific basin within the temperature ranges 15–20°C and 20–25°C, respectively. There is also a clear decrease in SS percentage in the Pacific basin at a similar depth of 3600 m for the 15–20°C range. For the 15–20°C range in the Indian and Atlantic Oceans (Figures 2e and 2f), there is no obvious tendency for higher RSP percentages with increasing depth. In this case the RSP alone cannot be used to determine a dissolution threshold. However, a decrease of SS species percentage with depth is observed in Figure 2e. This decrease indicates that dissolution might impact the assemblages at depths greater than ~3900 m. In the Indian Ocean for the 20–25°C range, both RSP increase and SS decrease with depth, suggesting a threshold of ~3800 m below which assemblages are impacted by dissolution. For the Southern Ocean (0–10°C, Figure 2c), cores retrieved at depths shallower than 3600 m show RSP percentages <30% and only four deeper cores display higher RSP percentages. Occasionally, we observe relatively shallow cores with higher RSP percentages (e.g., Figures 2c, 2d, 2e, 2f, 2g, 2i, and 2k, at ~1000 m, ~3000 m, ~50 m, ~1000 m, ~800 m, ~1000 m, and ~2900 m, respectively). Their relatively high RSP percentages suggest that all these cores, despite their shallow depths, have been affected by dissolution, or some other process, that has resulted in a biased foraminiferal assemblage. Thus, we discarded them from the SHO database.

From Figure 2, there is no unique depth at which the planktonic foraminiferal assemblages start to be affected by dissolution in the core tops. This is expected as the calcite saturation horizon ($\Delta\text{CO}_3^{2-} = 0$) is at different depths in the different basins due to deep ocean circulation. In the Atlantic Ocean, we do not see an impact of dissolution in the range 25–30°C where cores are mainly bathed by the North Atlantic Deep Water, characterized by a high ΔCO_3^{2-} concentration. At higher latitudes (20–25°C range) the impact of dissolution starts at depths >4300 m, where the ΔCO_3^{2-} decreases to ~0 $\mu\text{mol/kg}$. In the Indian Ocean

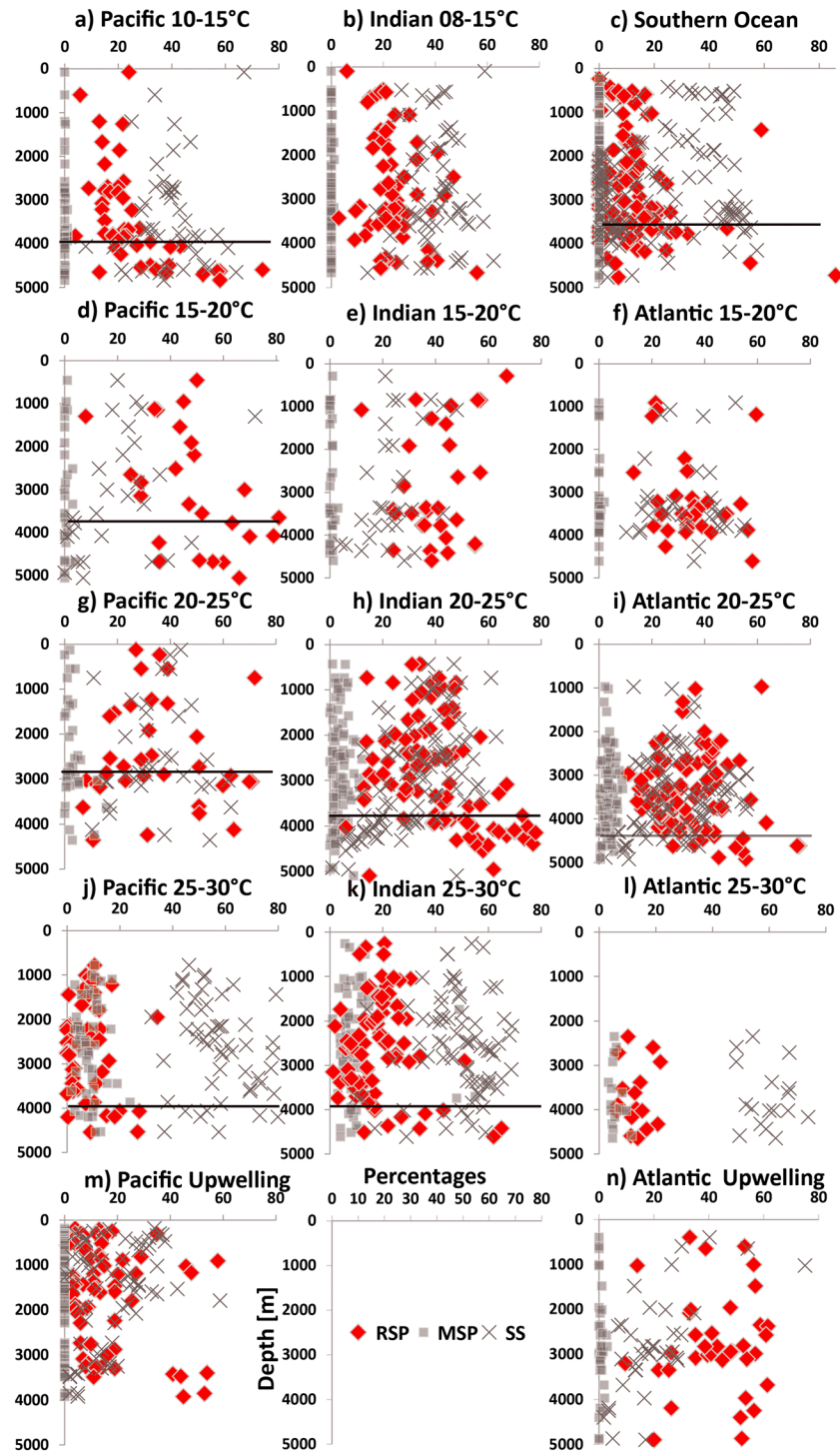


Figure 2. Plots of the percentages of the dissolution-sensitive species, SS (crosses); moderately sensitive species, MSP (squares); and dissolution-resistant species RSP (diamonds). Plots are separated according to different basins and summer SST ranges. The horizontal dark bars represent the depth threshold we chose in each case.

dissolution is evident for the temperature ranges 20–25 and 25–30°C (Figures 2h and 2k) at depths >3900 m. This corresponds to a maximum ΔCO_3^{2-} value of $\sim -6 \mu\text{mol/kg}$. In the Pacific Ocean, both RSP and SS percentages indicate dissolution occurring at depths >4000 and 3600 m in the midlatitudes for the temperature ranges 10–15 and 15–20°C, respectively.

When looking at core tops that have been discarded for dissolution from Figure 2 plots (supporting information Figure S1), it is clear that the RSP percentage starts to increase when the $\Delta\text{CO}_3^{2-} \leq \sim 0$ to $-5 \mu\text{mol/kg}$ in each basin in the 20–25°C ranges, $< \sim -5 \mu\text{mol/kg}$ in the Pacific and Indian Oceans for the 25–30°C ranges, and $< \sim -10 \mu\text{mol/kg}$ for the $< 20^\circ\text{C}$ ranges in the Pacific, Indian, and SO.

Species living in the deeper part of the water column generally contribute significantly to RSP, while shallow dwelling species are mainly included in SS. Unfortunately, this method cannot separate the dissolution signal from variations in the ratio between shallow and deep dwelling species. However, the clear depthwise increase of the RSP percentages indicates that, at least at higher dissolution rates, the dissolution signal overcomes this convolution. To further test the core-top foraminiferal assemblages for the effects of dissolution, we looked at transects of core tops in each basin, to determine at what depth the dissolution starts biasing the faunas. We chose regions where there are transects of core tops covering a relatively small area, which are distal from oceanographic fronts, to avoid concomitant SST changes, which might distort the dissolution signal. As different cores within each transect should display similar assemblages, any observed compositional differences should be directly linked to dissolution at the deeper core sites. We compared dissimilarity coefficients between the different core tops along each bathymetric transect and compared them to the depth profile of ΔCO_3^{2-} at their location (supporting information Figures S2 and S3).

For the first transect located in the southeast Atlantic (Figure 3a), amongst the six cores, only the deepest one displays an assemblage with an increased dissimilarity coefficient compared to the other shallower cores in the transect. The dissimilarity increases from ~ 0.04 between the shallowest cores to 0.12 for the deepest one. The clear increase in dissimilarity indicates that the assemblage of the deepest core site is influenced by a different factor from the other shallower cores. Thus, this indicates that, in the southeast Atlantic, species-selective dissolution starts to modify the planktonic foraminiferal assemblages between 4100 and 4400 m depth. This supports the carbonate dissolution threshold of ~ 4300 m, as defined above (Figure 2i).

The second transect, located in the SEP (Figure 3b), uses 10 cores. For cores shallower than 4100 m the dissimilarity between assemblages is generally lower than 0.2, while it increases to more than 0.4 between the core retrieved above 4100 m and cores from 4240 and 4550 m depth. When comparing the faunal content of all these sites, we observe that the two core tops at 4240 and 4550 m depth present the highest percentages of *G. truncatulinoides* (11 and 18%, compared with 4 to 7% for the shallower cores). This species is considered relatively dissolution resistant [Cullen and Prell, 1984]. However, for this transect, the deepest core-top assemblage at 4660 m depth is similar to that observed in cores shallower than 4100 m and not to that of the two closest core tops at 4240 and 4550 m depth. This suggests that the assemblage of the deepest core top is less affected by dissolution relative to the other deep core tops. The reason for this is unclear, but this observation may be due to lower organic matter export at this deepest core site or increased sedimentation rates at the deepest core compared to the other deep cores, generating different states of preservation. This transect indicates that, in the SEP, dissolution starts to modify the planktonic foraminifera assemblages between 4100 and 4200 m, slightly deeper than the depth of 4000 m indicated in Figure 2a for the corresponding temperature range.

The final transect is from the western tropical Indian Ocean (Figure 3c), using 15 cores. The core at 4425 m depth has an assemblage significantly different from the other core tops in this transect, with the highest percentage of the dissolution-resistant species *G. inflata* (27%). The percentage of this species varies in the other cores from 1 to 2% for the shallowest (< 3800 m) and from 6 to 27% for the deeper cores (> 3800 m). The shallower cores from this transect have a RSP percentage $< 13\%$, except for the 2833 m depth core, that shows a high dissimilarity value (0.2) when compared to the other shallow core tops (< 3800 m) (Figure 3c). The RSP percentage for the cores > 3800 m varies from 13 to 34%, with the lowest value of 13% paradoxically obtained in the deepest core, which might explain why it shows a relatively low dissimilarity coefficient (0.115 to 0.212) when compared to the shallowest five cores (Figure 3c, the light gray group of bars for this core). Generally, in the Indian Ocean, the dissimilarity coefficient transition between shallow, unbiased core tops and deep dissolution-biased core tops is not as sharp as in the other transects. For cores < 3800 m, the dissimilarities in their assemblages (lighter grey bars) are generally lower than the dissimilarities observed for the deeper cores (> 3800 m) (darker grey bars). The assemblage of the core located at 3654 m displays similar dissimilarities to both deep and shallow core-top assemblages. Conversely, for cores retrieved at depths > 3800 m, dissimilarities (dark grey bars) are generally lower than those recorded in the shallower

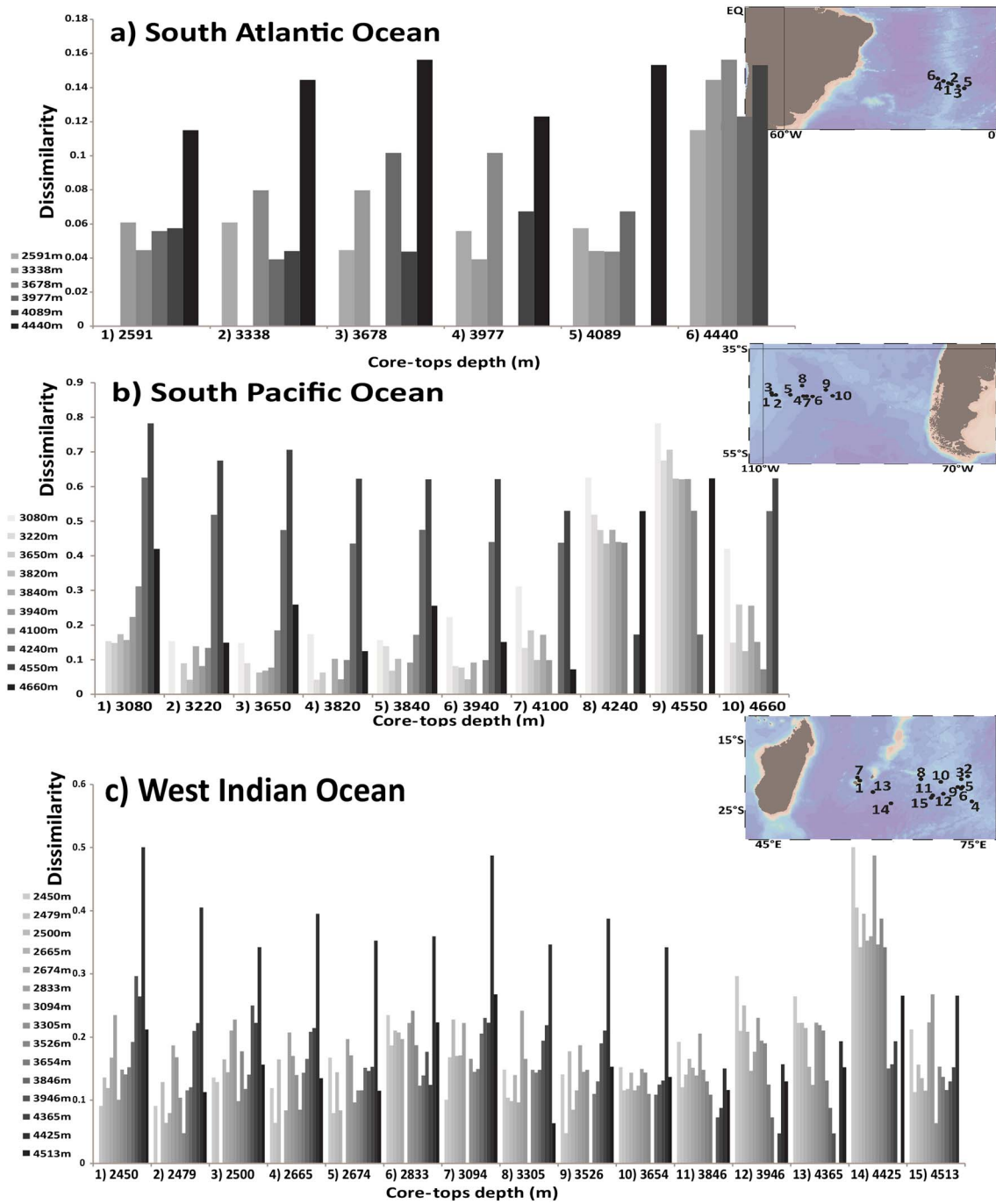


Figure 3. Bathyal transects of dissimilarity: Core tops on the x axis are sorted by water depth. The dissimilarity values obtained when assemblages of each core top are compared with the other core tops from the transect are represented by the columns, also sorted by water depth. Each column corresponds to the dissimilarity of the core with the other cores from the transect; the empty column represents the depth of the core itself.

cores (Figure 3c). These observations indicate that assemblages are biased by dissolution from around 3700–3800 m depth. This is slightly shallower than the depth of 3900–4000 m indicated for the subtropical Indian Ocean in Figures 2h and 2k.

Combining all the observations presented in this section, we propose a modern contextual depth threshold for the different basins (Table 1). We propose a threshold of 3800 m ($\Delta\text{CO}_3^{2-} = \sim -5$ to $-10 \mu\text{mol/kg}$) for core tops from the South Pacific and South Indian, 4000 m ($\Delta\text{CO}_3^{2-} = \sim -5$ to $-10 \mu\text{mol/kg}$) for the subtropical

Table 1. Contextual Depth and ΔCO_3^{2-} Threshold for the Different Basins

Basin/Region	Depth Threshold (m)	ΔCO_3^{2-} Threshold ($\mu\text{mol/kg}$)
South Pacific	3800	~ -5 to -10
South Indian	3800	~ -5 to -10
Subtropical Pacific	4000	~ -5 to -10
Subtropical Indian	4000	~ -5 to -10
South Atlantic	4200	~ 0 to -5
Subtropical Atlantic	4700	~ 0 to -5

Pacific and subtropical Indian Oceans, 4700 m ($\Delta\text{CO}_3^{2-} = \sim 0$ to $-5 \mu\text{mol/kg}$) for core tops from the subtropical Atlantic, and 4200 m ($\Delta\text{CO}_3^{2-} = \sim 0$ to $-5 \mu\text{mol/kg}$) for the South Atlantic Ocean. Furthermore, we suggest that care is taken whenever the ΔCO_3^{2-} value is near $\sim -5 \mu\text{mol/kg}$, regardless of the basin or the latitude. Faunal investigation is recommended as the assemblage starts to be suspicious once the RSP percentage is $>30\%$ in most of the core tops in the $25\text{--}30^\circ\text{C}$ [Cullen and Prell, 1984] and $10\text{--}15^\circ\text{C}$ ranges, in RSP percentages $>40\text{--}50\%$ in the $15\text{--}25^\circ\text{C}$ range (midlatitude areas with transitional fauna), and in zones of high organic matter fluxes.

Using this approach, based on RSP percentages and ΔCO_3^{2-} values, we identified and removed 184 dissolution-biased core tops from the new combined SHO database (supporting information Table S3).

2.2.1. Upwelling Zones Core Tops

It has previously been suggested that the faunal composition of planktonic foraminifera might be less dependent on SST in coastal upwelling areas due to the overriding effect of increased nutrient supply and drastically different water column structure [Ottens, 1991; Lombard et al., 2011], thus affecting the dissimilarity and biasing the temperatures obtained from these MAT methods. Here we identify two regions of upwelling and high productivity that may affect the underlying core-top assemblages: (i) the upwelling region along the Chilean margin, from 15°S down to 40°S , lowering the SST up to 100 km off the coast [Tomczak and Godfrey, 2003], and (ii) the Namibia upwelling system off the west coast of Africa, from 20°S to $\sim 37^\circ\text{S}$ [Tomczak and Godfrey, 2003]. These core tops were not discarded from our database but were instead flagged, and, if they were selected as analogs, their current oceanography was taken into consideration during the interpretation of the reconstructed SST (supporting information Table S2). We observe very high percentages of dissolution-resistant species in these upwelling zones (Figures 2m and 2n), which can be explained by either (i) an increased abundance of high productivity species such as *G. menardii flexuosa* [Cullen and Prell, 1984] or *N. dutertrei* [Bé and Tolderlund, 1971; Rohling and Gieskes, 1989] or (ii) increased dissolution bias at all depths due to more corrosive bottom water and pore water linked to higher organic matter fluxes in those regions. Due to the difficulty in separating between these two hypotheses, care needs to be taken during the SST reconstruction. The selection of these core tops as analogs may indicate specific ecological conditions and/or supralysocline dissolution events, both of which will strongly bias the SST estimates.

We used regional maps of RSP percentages to check if upwelling core tops indicate local trends (Figure 4). Cores from the Namibia upwelling system zone (Figure 4, top left), display high RSP percentages (orange dots along the African coast). In contrast, the core tops from the Chilean margin upwelling zone do not display high RSP values (Figure 4, bottom right).

These maps (Figure 4) also identify core tops showing odd RSP percentages that have no link with the local oceanography. This is the case for a core top in the Pacific Ocean at 30°S , 115°W (Figure 4, bottom left) and one located along the southeast Australian coast (Figure 4, top right), both characterized by a RSP of $>60\%$. We also note that two cores southeast of Cape Agulhas also show similarly high RSP percentages. These latter core tops are under the influence of the Agulhas Current, which has characteristic assemblages dominated by the subtropical species *G. ruber*, *G. sacculifer*, *G. siphonifera*, *G. glutinata*, *O. universa*, *G. menardii*, and *G. hexagona* [Peeters et al., 2004]. However, these two core tops also contain high percentages of the dissolution-resistant *G. inflata*, indicating that they might be biased by dissolution. We have discarded these core tops that have very different assemblages from the neighboring cores.

3. Database Validation

In order to validate our new database, we performed a “leave-one-out” reconstruction of the modern SST (World Ocean Atlas 1998 “WOA98” interpolated 10 first meters) first by using the whole SHO database

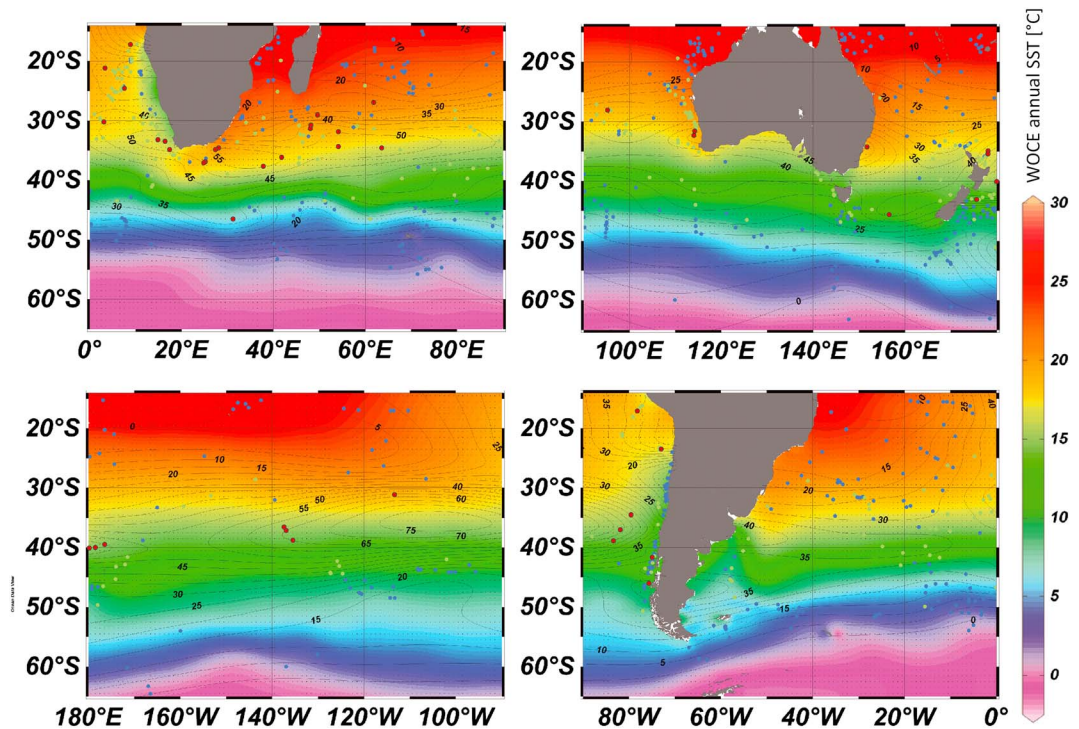


Figure 4. Annual mean World Ocean Circulation Experiment SST maps. The dots' colors represent RSP percentage ranges of the core tops: 0–30% in blue; 30–60% in green; and >60% in red. Contours represent the RSP percentages values for each of the core tops in the compiled database. Background colors represent annual SST. This map was created using Ocean Data View (ODV) with DIVA gridding [Schlitzer, 2015].

(Figure 5a), and then by running a second test after the removal of the deep, potentially dissolution-biased core tops (Figure 5b). These tests use a MAT calculation of the SST of each database core top by using the remaining data set. We used the BIOINDIC package developed by Joël Guiot and Yves Gally (CEREGE, CNRS, <https://www.eccorev.fr/spip.php?article389>), in R software [R Development Core Team, 2010]. The reconstructed annual SST is plotted against WOA98 SST (Figures 5a and 5b). On both graphs, the regression is close to a 1/1 slope with a very high coefficient of correlation ($r^2 = 0.97$). The cores are centered on this line from 2°C to 25.5°C, indicating the optimal range for the SST reconstruction. Reconstructions of SST <2°C is unreliable as the assemblages at these SST are composed of >95% of *N. pachyderma* left coiling. The remaining 5% of the assemblages are not diverse enough to reconstruct the 0–2°C SST range [Waelbroeck et al., 1998]. At SST >25.5°C the relationship appears nonlinear and is also erratic (probably due to a similar problem of only a few warmer species present). After removing cores <2°C and >25.5°C, we get a linear regression of $Y = 0.9862 (\pm 0.0068) X + 0.1744 (\pm 0.1134)$. The result of the test (Figure 5b) shows that the $\Delta_{SST}^{\text{observed-calculated}}$ is less than 2.7°C with the exception of 20 core tops. We put aside 12 outliers as their Δ_{SST} (the annual or seasonal) values were greater than 3 times the difference between the first and third quartiles. None of these core tops possess chronological information; thus, they could be either from the early Holocene (>8000 years, with potentially higher than modern SST) or from the last glacial or deglaciation period (lower than modern SST). The supporting information Figure S5 indicates the variation in residuals before and after removing the deep core tops from the database. We note higher residuals (>4°C) at higher depths (and lower ΔCO_3^{2-}) when leaving the deep core tops in the database, indicating the extent of the dissolution-bias introduced in the SST reconstructions. This supports the idea that these deep core tops should be discarded from the database and that SST reconstructions on dissolution-biased downcore samples should be avoided. To summarize, we removed 204 cores from the original compiled database of 802 core tops. The main factor for removing core tops was their depth and low ΔCO_3^{2-} values (supporting information Table S3 includes the reasons for removing each core top). Thus, the final database contains 598 core tops (supporting information Table S4). Tests on the new database allowed us to obtain a root-mean-square error (RMSE) of 1.00°C and error of $1\sigma = 0.89^\circ\text{C}$ for annual SST reconstructions (Table S5 in supporting information displays the seasonal errors). This is an

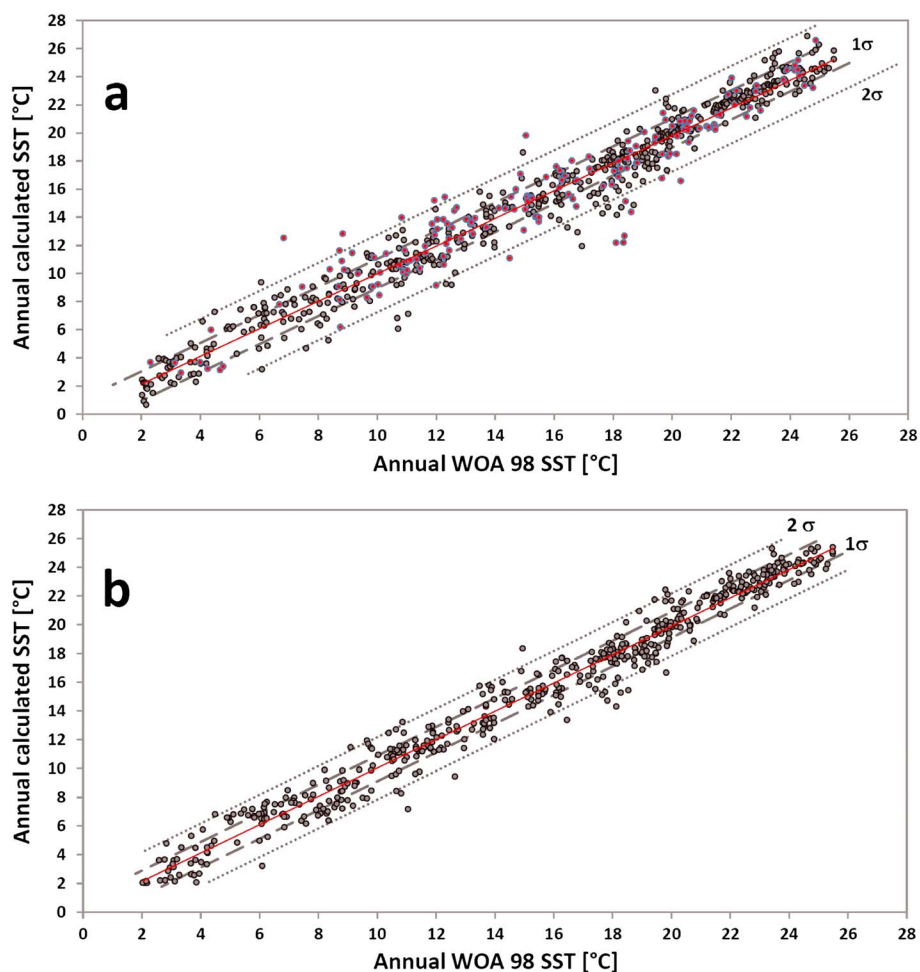


Figure 5. Leave-one-out validation tests of our database for annual temperature reconstruction. (a) The database with deep core tops and (b) the database without dissolved, deep core tops. In Figure 5a, these last core tops are shown as red dots. The dotted lines represent the 1σ error (1.04°C and 0.89°C for Figures 5a and 5b, respectively), and dots and lines correspond to 2σ (2.76 and 2.07°C for Figures 5a and 5b, respectively) to emphasize the outliers.

improvement on other databases such as the MARGO database where the mean (RMSE) for annual reconstructions over the South Atlantic and the Pacific basins was 1.51°C [Kucera *et al.*, 2005a]. The removal of the deep biased cores results in a small, but significant, reduction of the residuals by 0.1 to 0.2°C (supporting information Table S5 and Figures 5a and 5b).

This new database is open to the addition of further core tops, and we hope the SHO database will continue to develop. However, we recommend carefully checking the chronology and dissolution biases of their core tops prior to adding them to the database. RSP and SS percentages should also be checked, and if the ΔCO_3^{2-} at the location of the core is $< \sim -5$ to -10 $\mu\text{mol/kg}$ in the Indian and Pacific oceans and < 0 to -5 $\mu\text{mol/kg}$ in the Atlantic Ocean, the core top should not be added to maintain the quality of the database for paleo-SST reconstructions. Furthermore, if new chronological data on the core tops are produced, and it appears that the ages are not Holocene, they should be removed from the SHO database.

4. Paleo-application of the SHO Database: MD07-3100 Core

We used the new database to reconstruct the paleo-SST for a long CALYPSO core (MD07-3100; 1609 m; 41°36' S, 74°57'W; 29.83 m, modern summer SST 15.5°C) which was retrieved from the SEP during the PACHIDERME (Pacifique Chili Dynamique des Eaux intermédiaires) campaign on the R/V *Marion Dufresne* [Kissel, 2007]. This core is positioned south of the subtropical front (STF), in a region where previous databases did not contain

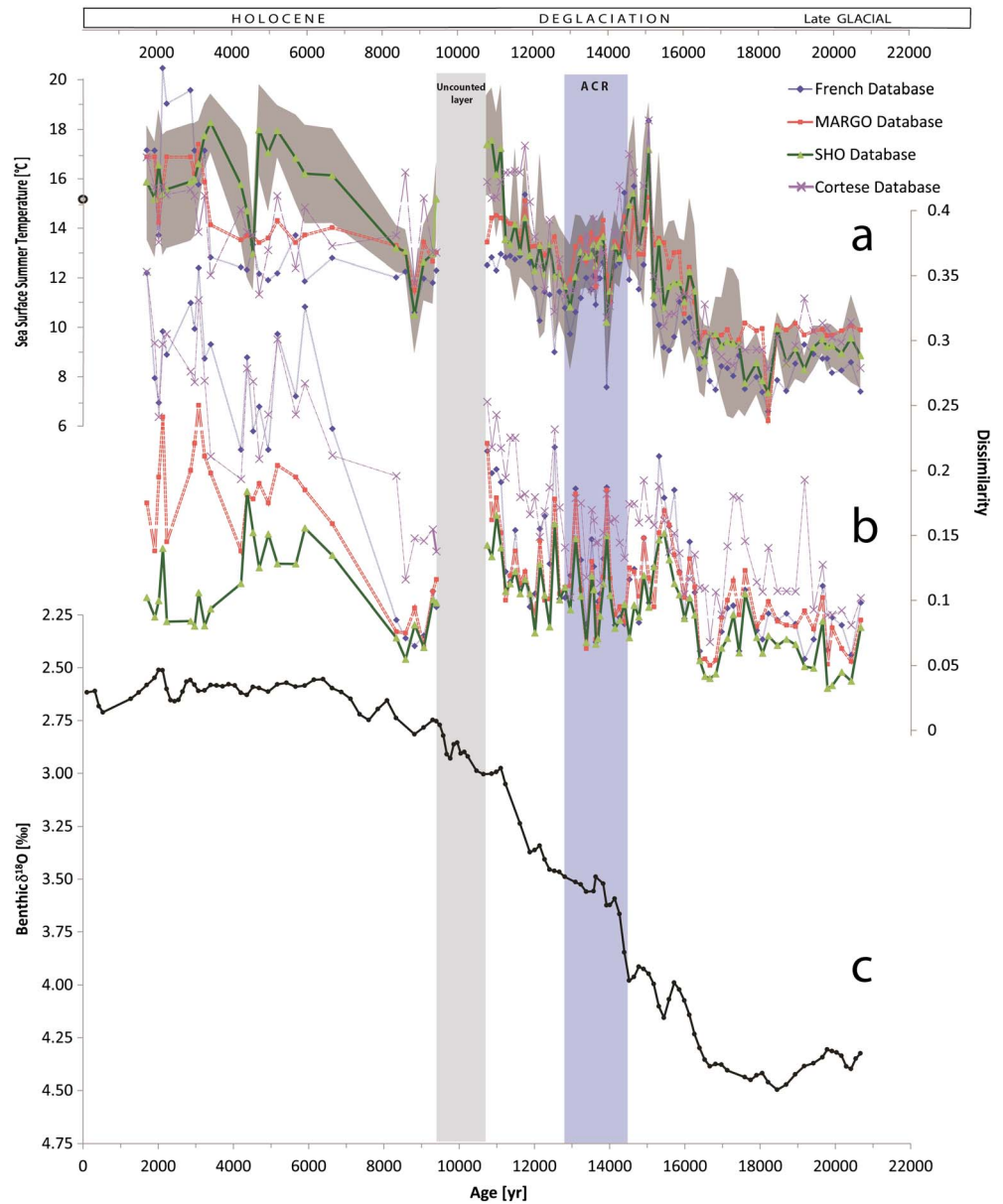


Figure 6. Test of the different databases on core MD07-3100. (a) SSST reconstruction using the different databases, grey envelope represents the error (1σ) of the reconstruction using the new SHO database. The dot represents the actual SSST at the location of the core. The light grey vertical bar indicates the Antarctic Cold Reversal from 14.5 to 12.8 ka [Lemieux-Dudon et al., 2010]. (b) The dissimilarity of each level. (c) The $\delta^{18}\text{O}$ curve measured on benthic foraminifera *Cibicides* spp. from this core, providing a chronological time frame.

good core-top coverage (Figure 1). We compare the paleo-SST obtained by the MAT method on 92 downcore samples, using the three original databases and our new SHO database, highlighting the influence of having core tops in the close vicinity of the MD07-3100 core, as well as the impact of dissolution-biased analogs. The focus of this paper is on the comparison between the different foraminifera assemblage MAT SST reconstructions, with only a brief reference to paleoclimatic features.

We reconstructed summer sea surface temperatures (SSST) for the first 14.8 m of the core (Figure 6a) using the Paleoanalog program [Therón et al., 2004]. We chose SSST, as along with spring, it is the main season for phytoplankton blooms in this area, and when we compare the different reconstructed seasonal SST, they display a constant seasonal SST offset (supporting information Figure S3). In contrast to previous studies, we did not use a dissimilarity threshold cutoff [Overpeck et al., 1985; Prell, 1985; Kallel et al., 2000]; instead, we kept

5 to 11 analogs, i.e., the first best analogs before any sharp increase of the dissimilarity of the first 15 best analogs, as described in *Waelbroeck et al.* [1998].

The stratigraphy of the core was based on the benthic foraminiferal $\delta^{18}\text{O}$ record analyzed on *Cibicidoides* spp. (Figure 6c) and compared to the benthic foraminiferal $\delta^{18}\text{O}$ in the nearby well-dated core MD07-3088 [*Siani et al.*, 2013], which sits at a similar water depth, the transition between Antarctic Intermediate Water and Pacific Central Water (supporting information Figure S4). The MD07-3100 core has high sedimentation rates of 60–100 cm/ka for the top 14.8 m, with no obvious hiatuses, providing a detailed record of the late glacial period, the deglaciation, and the Holocene. The four SSST records reconstructed using the different databases generally show good agreement (Figure 6c).

Between 6 and 7.25 m, we note the presence of a layer containing high amounts of volcanic particles (tephra) with diluted foraminiferal content. Thus, the counts from this interval are on <300 foraminifera, rendering any paleo-SSST reconstruction for this interval less reliable. The foraminifera fragments were also counted, to check for evidence of past increases in dissolution due to decreases in the $[\text{CO}_3^{2-}]$ of the waters at the core site (supporting information Figure S6a). All samples have $\leq 10\%$ fragments, which is a rather low percentage. The RSP percentages vary from 0.7 to 39% (supporting information Figure S6b). The RSP percentages are lower than 25–30% when the temperatures are lower than 15°C, which is similar to the values in Figure 2a. Only a few points of RSP percentages exceed 23%, while the depth where RSP reaches 39% corresponds to a period of relatively high temperatures ($\sim 15^\circ\text{C}$). This is not uncommon for the Pacific for the temperature range 15–20°C (Figure 2d). The 39% RSP also corresponds to the second highest fragment content ($\sim 9\%$); the warm reconstructed temperature is coherent with the warm temperature reconstructed for this time interval. So we consider it unlikely that there were any dissolution events that affected the downcore foraminiferal assemblages.

4.1. Late Glacial

The glacial temperatures extend to 16.5 ka in this core. The French database reconstructions are the coldest (SSST ranging from 6 to 9°C), whereas MARGO database results in slightly warmer estimates (SSST ranging from 6 to 11°C). The MARGO SSST estimates are also the most stable (9.5–10°C) during the late glacial period, while the three other SSST reconstructions show greater short-term variability. A cold period, with the coldest values (7.5–8°C), is indicated by SHO and the French database between 18.3 to 17.5 ka, while the two other databases indicate just one cold point at 18.3 ka. During the late glacial, dissimilarities are low (≤ 0.15) with the largest ones obtained using the MARGO database (up to 0.2), while the SST error bars (the direct result of SST differences between the best analogs) are lowest using the SHO database (up to 1.3°C) (supporting information Table S6).

4.2. Deglaciation

The onset of the last deglaciation starts at ~ 16.5 ka in core MD07-3100, with increasing SSST and declining $\delta^{18}\text{O}$ values (Figure 6a). An increasing SSST trend is observed from ~ 16.5 to 15 ka, reaching a maximum of 18°C at around 15 ka. This warming phase is followed by a SSST decrease (of 5°C on average across all databases) from 15 to 14.2 ka, then by a period during which temperatures show values varying from 14.5°C to 12°C between 14.2 and 12 ka. This first cooling is marked by a two-step oscillation of SSST, with lowest temperatures obtained by all of the databases at around 13.8 ka. From 14.2 to 12 ka, the SSST signals are more scattered, with one common cold event from 13.2 to 12.5 ka (magnitude larger than 2°C).

We interpret that the beginning of the deglaciation corresponds to a first warming, with high SSST recorded by all four databases at around 15 ka, just before a marked cooling period ($\sim 5^\circ\text{C}$ SSST decrease observed in all the databases) that likely corresponds to the Antarctic Cold Reversal (ACR) [*Pedro et al.*, 2015]. This warm event prior to the ACR has previously been observed in the southeast Atlantic and is characterized by high percentages of warm planktonic species [*Barker et al.*, 2009]. The transition to the Holocene is marked by a final warming event common in all the four SSST reconstructions, which occurs from 12 to 11 ka.

Dissimilarity values during the deglaciation are higher (by ~ 0.1 on average for all the reconstructions, with the largest dissimilarities obtained by the MARGO database) than for the late glacial. The error bars increase slightly to $\sim 1.9^\circ\text{C}$ during the deglaciation for the SHO database, while those associated with the Cortese database are higher by 1°C on average. The error bars for the French and MARGO databases are lower by 0.6°C during the deglaciation.

4.3. Holocene

The highest reconstructed SSST (17.5°C) are reached at the beginning of the Holocene using the SHO database. The SSST reconstruction >17°C probably indicates a southward shift of the STF during the early Holocene as suggested by studies on dinoflagellate cysts assemblages from the adjacent Ocean Drilling Program core 1233 [Verleye and Louwye, 2010]. Lower SSST are estimated (~13–14°C) by the other databases. During the middle to late Holocene the SSST reconstructed by the four databases diverge (Figure 6a). At 7 ka SSST obtained from the new SHO database increase again, up to 18°C at ~5 and ~3 ka. These two warming phases are separated by a cold SSST event at around 4.5 ka with SSST values down to ~13°C. The reconstructed SSST based on the SHO database starts decreasing from 3 to 1.5 ka, reaching a SSST of 15.5°C after 1.5 ka, similar to the modern SSST value (WOA98). The SSST increase from the other databases lags by 4 ka. Using the French database, the increase starts at 3 ka reaching a maximum >19°C, while the MARGO database displays a plateau of 17°C from 3 to 2 ka, and the Cortese database displays a progressive increase of the SSST during this interval, with SSST reaching a maximum of 17°C at 2 ka.

The reasons for these considerable discrepancies between the databases can be investigated by looking at the dissimilarity curves (Figure 6b). During the warm Holocene events (around 11 ka and between 7 and 1.5 ka), there are significant differences in the dissimilarities of the new SHO database and the other databases. Dissimilarities reach a maximum (up to 0.3–0.35) during these events, except for the SHO database (always ≤0.2). This is most likely due to the lack of core tops in the SEP in the French and MARGO databases, when SEP core tops are the only analogs chosen for the SSST reconstruction using the SHO database (from 11 to 10.8 ka and 3.1 to 1.5 ka). We suggest that the high dissimilarities during this interval using the Cortese database, which does contain SEP core tops, is likely due to the inclusion of dissolution-biased deep core tops and/or very shallow core tops, which have been discarded in the new compiled SHO database. The late Holocene has the largest error bars, reaching approximately 2.2°C from 1.5 to 3 ka for the SHO database, with larger errors documented for the Cortese, MARGO, and the French databases, which display errors of 3.4°C, 2.7°C, and 2.9°C, respectively. These larger error bars during the Holocene period are possibly linked to the vicinity of the subtropical front and its interannual latitudinal variability. This behavior will be discussed in a paleoceanographic paper with latitudinal reconstructions of the SST along the Chilean coast.

4.4. Reconstruction Quality

The late glacial and the deglaciation show less interdatabase discrepancy in terms of error bars, with the majority of the SSST values within the error range of the new SHO database (Figure 6a, grey envelope). The exceptions to this are a couple of SSST estimates using the MARGO database. The late glacial also displays the lowest dissimilarities (below 0.2). This is likely due to the fact that late glacial SSST of 7 to 8°C is characteristic of the modern sub-Antarctic Front, and there are no core tops available in any of the databases south of this front in Drake Passage. Thus, during the late glacial period, the analogs used for the SSST reconstruction are core tops mainly from the South Atlantic and South Indian Oceans. This is probably not an issue as it is likely that the ACC homogenizes the fauna at these latitudes as indicated by the low dissimilarities obtained.

In contrast, during the Holocene, the SSST reconstructions using the different databases behave very differently from each other, and the differences are often larger than the error bars (sum of 1σ for the different reconstructions). When we look at the dissimilarity values recorded, the most reliable reconstructions are using the new SHO database (dissimilarities <0.2), especially during the late Holocene, where the analogs are from the surrounding SEP region indicating that modern conditions have been achieved.

5. Conclusions

We established a new core-top database for the Southern Hemisphere oceans (SHO), combining three existing databases and investigating the dissolution biases that can affect their faunal census counts. This new database is able to reconstruct past SSST variations from 2° to 25.5°C. Validation tests on this new database have shown an error at 1σ of 0.89°C for the annual SST.

We hope that this database will continue to develop, and we encourage potential users to add new core tops from additional locations, as long as ΔCO_3^{2-} thresholds are taken into consideration to avoid dissolution biases. We recommend a threshold of 3800 to 4000 m/ $\Delta\text{CO}_3^{2-} = \sim -10$ to $-5 \mu\text{mol/kg}$ for the Pacific and Indian Oceans and 4200 to 4700 m/ $\Delta\text{CO}_3^{2-} = \sim 0$ to $10 \mu\text{mol/kg}$ for the Atlantic Ocean (Table 1). We also

recommend that the core-top foraminiferal census count is checked for the RSP and SS percentages before adding it to the database. It is also important that any ecologic specificity (e.g., upwelling zone) is noted. Moreover, when reconstructing past SSST changes, we recommend that the number of analogs chosen takes into account the dissimilarity increase with increasing analogs. We also recommend that SSST reconstructions are not attempted for time intervals during which the cores may have been affected by dissolution, as the results will be unreliable. In this respect, a series of quantitative measures (e.g., core-top communality value for the Imbrie and Kipp Transfer Function, and Foraminifera Fragmentation Index) should, where available, be provided in order to flag potentially biased core tops/downcore samples and thus help in discarding samples impacted by dissolution. We recommend that SST reconstructions are not attempted for time intervals during which the cores may have been affected by dissolution, as the results will be unreliable.

This database allowed the reconstruction of SSST since the late glacial on a marine core from the SEP. The paleo-SSST reconstruction was performed using different calibration databases in order to highlight how biases affecting assemblages in the databases influence the reconstructed SSST curves. Indeed, the different temperature reconstructions indicate different behavior during the middle to late Holocene, with temperature differences larger than the error of the reconstructions (1σ). Faunal dissimilarity is a good indicator of the validity of the SSST reconstruction; however, choosing a constant threshold of 0.25 is not reliable, as indicated by opposite trends for MARGO and SHO database SSST reconstructions for the late Holocene with dissimilarities always ≤ 0.25 . Using the new SHO database presented in this paper, the SSST reconstruction displayed constant low dissimilarities, suggesting that this is the most reliable SSST reconstruction.

The most crucial aspect we would like to stress when assembling modern data sets to be used as proxy for paleo-SST is the importance of a bias-free and geographic-rich database, in which quality is preferred to quantity. The SHO database is open to further additions of core tops which have been quality checked for census and chronological framework. If absolute age information become available for any core tops after their inclusion in this database, and if such data should suggest that they are not <8000 years (middle Holocene or younger age a time interval when modern sea level and oceanographic conditions were reached), we advise that they are removed.

Acknowledgments

We thank all the individuals who have contributed core-top foraminiferal assemblage counts to all of these databases. We thank the captains and the crew of the R/V *Marion Dufresne* during the PACHIDERME voyage for their help retrieving the MD-3100 core and Fabien Dewilde for performing the stable isotope measurements on this core. Comments by Franck Bassinot, Jean-Claude Duplessy, and Claire Waelbroeck helped to improve this manuscript. We also thank Annachiara Bartolini and a second anonymous reviewer for the very helpful and interesting comments that helped to greatly improve the manuscript. Financial support was made by the French Ministry of Research and Higher Education and the French-Swedish project on SO VR-349-2012-6278. Supporting data are included as six tables in a supporting information file; the SHO database can also be obtained from PANGAEA (<https://www.pangaea.de>). The contribution number of the LSCE Laboratory is 5742.

References

- Arrhenius, G. (1952), Sediment cores from the East Pacific Reports of the Swedish Deep-Sea Expedition 1947-19485, 1–228.
- Aurahs, R., Y. Treis, K. Darling, and M. Kucera (2011), A revised taxonomic and phylogenetic concept for the planktonic foraminifer species *Globigerinoides ruber* based on molecular and morphometric evidence, *Mar. Micropaleontol.*, **79**, 1–14.
- Bard, E. (2001), Comparison of alkenone estimates with other paleotemperature proxies, *Geochem. Geophys. Geosyst.*, **2**(1), doi:10.1029/2000GC000050.
- Barker, S., P. Diz, M. J. Vautravers, J. Pike, G. Knorr, I. R. Hall, and W. S. Broecker (2009), Interhemispheric Atlantic seesaw response during the last deglaciation, *Nature*, **457**(7233), 1097–1102, doi:10.1038/nature07770.
- Bé, A. W. H. (1977), An ecological, zoogeographic and taxonomic review of recent planktonic foraminifera, in *Oceanic Micropaleontology*, vol. 1, edited by A. T. S. Ramsay, pp. 1–100, Academic Press, London.
- Bé, A. W. H., and D. S. Tolderlund (1971), Distribution and ecology of living planktonic foraminifera in surface waters of the Atlantic and Indian Oceans, in *The Micropaleontology of Oceans*, edited by B. M. Funnel and W. R. Riedel, pp. 105–149, Cambridge Univ. Press, London.
- Berger, W. H. (1970), Planktonic foraminifera: Selective solution and the lysocline, *Mar. Geol.*, **8**, 111–138.
- Brassell, S. C., G. Eglinton, I. T. Marlowe, U. Pflaumann, and M. Sarnthein (1986), Molecular stratigraphy: A new tool for climatic assessment, *Nature*, **320**(6058), 129–133, doi:10.1038/320129a0.
- Broecker, W. S., and T. Takahashi (1978), Relationship between lysocline depth and in situ carbonate ion concentration, *Deep Sea Res.*, **25**(1), 65–95.
- Caley, T., D. M. Roche, C. Waelbroeck, and E. Michel (2014), Constraining the Last Glacial Maximum climate by data-model (iLOVECLIM) comparison using oxygen stable isotopes, *Clim. Past Discuss.*, **10**(1), 105–148, doi:10.5194/cpd-10-105-2014.
- Conkright, M. E., et al. (1998), World Ocean Database 1998, CD-ROM Data Set Documentation. O.C.L Natl. Oceanogr. Data Cent. Internal Rep. 14, 111.
- Cortese, G., et al. (2013), Southwest Pacific Ocean response to a warmer world: Insights from marine isotope stage 5e, *Paleocyanography*, **28**, 585–598, doi:10.1002/palo.20052.
- Cullen, J. L., and W. L. Prell (1984), Planktonic foraminifera of the northern Indian Ocean: Distribution and preservation in surface sediments, *Mar. Micropaleontol.*, **9**(1), 1–52, doi:10.1016/0377-8398(84)90022-7.
- Darling, K. F., and C. M. Wade (2008), The genetic diversity of planktonic foraminifera and the global distribution of ribosomal RNA genotypes, *Mar. Micropaleontol.*, **67**(3–4), 216–238, doi:10.1016/j.marmicro.2008.01.009.
- Darling, K. F., M. Kucera, C. J. Pudsey, and C. M. Wade (2004), Molecular evidence links cryptic diversification in polar planktonic protists to Quaternary climate dynamics, *Proc. Natl. Acad. Sci. U.S.A.*, **101**(20), 7657–7662, doi:10.1073/pnas.0402401101.
- de Vargas, C., R. Norris, L. Zaninetti, S. W. Gibb, and J. Pawlowski (1999), Molecular evidence of cryptic speciation in planktonic foraminifers and their relation to oceanic provinces, *Proc. Natl. Acad. Sci. U.S.A.*, **96**, 2864–2868.
- Imbrie, J., and N. G. Kipp (1971), A new micropaleontological method for quantitative paleoclimatology: Application to a late Pleistocene Caribbean core, in *The Late Cenozoic Glacial Ages*, edited by K. K. Turekian, pp. 71–181, Yale Univ. Press, New Haven, Conn.

- Kallel, N., J. C. Duplessy, L. Labeyrie, M. Fontugne, M. Paterne, and M. Montacer (2000), Mediterranean pluvial periods and sapropel formation over the last 200 000 years, *Palaeoogeogr. Palaeoclimatol. Palaeoecol.*, 157(1-2), 45–58, doi:10.1016/S0031-0182(99)00149-2.
- Kissel, C. (2007), *MD 159-PACHIDERME IMAGES XV, Cruise Report 06.02.07-28.02.07*, vol. 1, pp. 84, Institut Polaire Français Paul Émile Victor, Plouzané.
- Kucera, M., et al. (2005a), Reconstruction of sea-surface temperatures from assemblages of planktonic foraminifera: Multi-technique approach based on geographically constrained calibration data sets and its application to glacial Atlantic and Pacific Oceans, *Quat. Sci. Rev.*, 24(7-9), 951–998, doi:10.1016/j.quascirev.2004.07.014.
- Kucera, M., A. Rosell-Melé, R. Schneider, C. Waelbroeck, and M. Weinelt (2005b), Multiproxy approach for the reconstruction of the glacial ocean surface (MARGO), *Quat. Sci. Rev.*, 24(7-9), 813–819, doi:10.1016/j.quascirev.2004.07.017.
- Le, J., and N. J. Shackleton (1992), Carbonate dissolution fluctuations in the western equatorial Pacific during the late Quaternary, *Paleoceanography*, 7, 21–42, doi:10.1029/91PA02854.
- Lemieux-Dudon, B., E. Blayo, J. R. Petit, C. Waelbroeck, A. Svensson, C. Ritz, J. M. Barnola, B. M. Narcisi, and F. Parrenin (2010), Consistent dating for Antarctic and Greenland ice core, *Quat. Sci. Rev.*, 29(1), 8–20.
- Lombard, F., L. Labeyrie, E. Michel, L. Bopp, E. Cortijo, S. Retailleau, H. Howa, and F. Jorissen (2011), Modelling planktic foraminifer growth and distribution using an ecophysiological multi-species approach, *Biogeosciences*, 8(4), 853–873, doi:10.5194/bg-8-853-2011.
- Malmgren, B. A., and U. Nordlund (1996), Application of artificial neural networks to chemostratigraphy, *Paleoceanography*, 11(4), 505–512, doi:10.1029/96PA01237.
- Marshall, J., and K. Speer (2012), Closure of the meridional overturning circulation through Southern Ocean upwelling, *Nat. Geosci.*, 5(3), 171–180, doi:10.1038/ngeo1391.
- Mix, A. C., E. Bard, and R. Schneider (2001), Environmental Processes of the Ice age: Land, Oceans, Glaciers (EPILOG), *Quat. Sci. Rev.*, 20, 267–258.
- Niebler, H.-S., and R. Gersonde (1998), A planktic foraminiferal transfer function for the southern South Atlantic Ocean, *Mar. Micropaleontol.*, 34(3-4), 213–234, doi:10.1016/S0377-8398(98)00009-7.
- Nürnberg, D. (1995), Magnesium in tests of *Neoglobobulimina pachyderma* sinistral from high northern and southern latitudes, *J. Foraminiferal Res.*, 25(4), 350–368.
- Ottens, J. J. (1991), Planktic foraminifera as North Atlantic water mass indicators, *Oceanol. Acta*, 14(2), 123–140 Retrieved from papers2://publication/uuid/245EEE02-A562-4562-B9DA-850C910577C6.
- Overpeck, J. T., T. Webb, and I. C. Prentice (1985), Quantitative interpretation of fossil pollen spectra: Dissimilarity coefficients and the method of modern analogs, *Quat. Res.*, 23(1), 87–108, doi:10.1016/0033-5894(85)90074-2.
- Patterson, R. T., and E. Fishbein (1989), Determine the number of point counts needed for micropaleontological quantitative research, *Society*, 63(2), 245–248.
- Pedro, J. B., et al. (2015), The spatial extent and dynamics of the Antarctic Cold Reversal, *Nat. Geosci.*, 9, 51–55, doi:10.1038/ngeo2580.
- Peeters, F. J. C., R. Ancheson, G. J. A. Brummer, W. P. M. de Ruijter, R. R. Schneider, G. M. Gansen, E. Ufkes, and D. Kroon (2004), Vigorous exchange between the Indian and Atlantic oceans at the end of the past five glacial periods, *Nature*, 430, 661–665.
- Pflaumann, U., J. Duprat, C. Pujol, and L. D. Labeyrie (1996), SIMMAX: A modern analog technique to deduce Atlantic sea surface temperatures from planktonic foraminifera in deep-sea sediments, *Paleoceanography*, 11(1), 15–35, doi:10.1029/95PA01743.
- Phleger, F. B., F. L. Parker, and J. F. Peirson (1953), North Atlantic core foraminifera, *Rept. Swed. Deep Sea Exped.*, 7, 1–222.
- Prell, W. L. (1985), The stability of low-latitude sea-surface temperatures: An evaluation of the CLIMAP reconstruction with emphasis on the positive SST anomalies U.S. Dep. of Energy, 60.
- R Development Core Team (2010), *R: A Language and Environment for Statistical Computing*, R Foundation for Statistical Computing, Vienna, Austria. [Available at <http://www.R-project.org/>]
- Rohling, E. J., and W. W. C. Gieskes (1989), Late Quaternary changes in Mediterranean intermediate water density and formation rate, *Paleoceanography*, 4(5), 531–545, doi:10.1029/PA004i005p00531.
- Ruddiman, W. F., and B. C. Heezen (1967), Differential solution of planktic foraminifera, *Deep-Sea Res.*, 17, 801–808.
- Salvignac, M. E. (1998), Variabilité hydrologiques et climatique de l’océan Austral (secteur indien) au cours du Quaternaire terminal. Essai de corrélations inter-hémisphériques PhD thesis, Univ. de Bordeaux, 1, 354.
- Schlitzer, R. (2015), Ocean Data View. [Available at odv.awi.de]
- Schott, G. (1935), Die Foraminiferen aus dem äquatorialen Teil des Atlantischen Ozeans, *Deutsch Atlantica Exped. 'Meteor'*, 3, 34–134.
- Siani, G., E. Michel, R. De Pol-Holz, T. Devries, F. Lamy, M. Carel, G. Isiguer, and A. Laurantou (2013), Carbon isotope records reveal precise timing of enhanced Southern Ocean upwelling during the last deglaciation, *Nat. Commun.*, 4, 2758, doi:10.1038/ncomms3758.
- Therón, R., D. Paillard, E. Cortijo, J. A. Flores, M. Vaquero, F. J. Sierro, and C. Waelbroeck (2004), Reconstruction of paleoenvironmental features using a new multiplatform program, *Micropaleontology*, 50(4), 391–395.
- Thunell, R. C. (1976), Optimum indices of calcium carbonate dissolution in deep-sea sediment, *Geology*, 4, 525–528.
- Tomczak, M., and Godfrey, S. (2003), The Atlantic Ocean, in *Regional Oceanography: An Introduction*, vol. 2, 2nd ed., pp. 229–252, Daya, Delhi, India.
- Verleye, T. J., and S. Louwyck (2010), Late Quaternary environmental changes and latitudinal shifts of the Antarctic Circumpolar Current as recorded by dinoflagellate cysts from offshore Chile (41°S), *Quat. Sci. Rev.*, 29(7-8), 1025–1039, doi:10.1016/j.quascirev.2010.01.009.
- Volbers, A. N. A., and R. Henrich (2002), Late Quaternary variations in calcium carbonate preservation of deep-sea sediments in the northern Cape Basin: Results from a multiproxy approach, *Mar. Geol.*, 180(1-4), 203–220, doi:10.1016/S0025-3227(01)00214-6.
- Waelbroeck, C., L. Labeyrie, J. Duplessy, J. Guiot, M. Labracherie, H. Leclaire, and J. Duprat (1998), Improving past sea surface temperature estimates based on planktonic fossil faunas, *Paleoceanography*, 13(3), 272–283, doi:10.1029/98PA00071.